



Master's thesis  
Master's Programme in Atmospheric Sciences  
Meteorology

# Cumulonimbus cloud detection with weather radar at Helsinki-Vantaa airport

Laura Tuomola

March 22, 2021

Supervisors: Ph.D. Jussi Ylhäisi  
Prof. Heikki Järvinen

Examiners: Prof. Heikki Järvinen  
Dos. Marja Bister

UNIVERSITY OF HELSINKI  
FACULTY OF SCIENCE  
PL 64 (Gustaf Hällströmin katu 2a)  
00014 Helsingin yliopisto

Tiedekunta — Fakultet — Faculty Faculty of science		Koulutusohjelma — Utbildningsprogram — Degree programme Master's Programme in Atmospheric Sciences Meteorology	
Tekijä — Författare — Author Laura Tuomola			
Työn nimi — Arbetets titel — Title Cumulonimbus cloud detection with weather radar at Helsinki-Vantaa airport			
Työn laji — Arbetets art — Level Master's thesis		Aika — Datum — Month and year March 22, 2021	Sivumäärä — Sidantal — Number of pages 42
Tiivistelmä — Referat — Abstract <p>Cumulonimbus (Cb) clouds form a serious threat to aviation as they can produce severe weather hazards. Therefore, it is important to detect Cb clouds as well as possible. Finnish Meteorological Institute (FMI) provides aeronautical meteorological services in Finland, including METeorological Aerodrome Report (METAR). METAR describes weather at the aerodrome and its vicinity. Significant weather is reported in METARs, and therefore Cb clouds must be included in it. At Helsinki-Vantaa METARs are done manually by human observer. Sometimes Cb detection can be more difficult, for example, when it is dark, and it is also expensive to have human observers working around the clock all year round. Therefore, automation of Cb detection is a topical matter.</p> <p>FMI is applying an algorithm that uses weather radar observations to detect Cb clouds. This thesis studies how well the algorithm can detect Cb clouds compared to manual observations. The dataset used in this thesis contains summer months (June, July and August) from 2016 to 2020. Various verification scores can be calculated to analyse the results. In addition, daytime and night-time differences are calculated as well as different years and months are compared together. The results show that the algorithm is not adequate to replace human observers at Helsinki-Vantaa. However, the algorithm could be improved, for instance, by adding satellite observations to improve detection accuracy.</p>			
Avainsanat — Nyckelord — Keywords Meteorology, cumulonimbus, radar			
Säilytyspaikka — Förvaringsställe — Where deposited			
Muita tietoja — Övriga uppgifter — Additional information			

# Contents

<b>Acronyms</b>	<b>3</b>
<b>1 Introduction</b>	<b>4</b>
<b>2 Theory</b>	<b>6</b>
2.1. Convection . . . . .	6
2.2. Cumulonimbus cloud . . . . .	9
2.3. METAR . . . . .	12
2.4. Weather radar geometry . . . . .	14
<b>3 Data and methods</b>	<b>20</b>
3.1. Validation . . . . .	21
<b>4 Results</b>	<b>24</b>
4.1. Case examples . . . . .	30
4.2. Future steps . . . . .	36
<b>5 Conclusions</b>	<b>37</b>
<b>6 Acknowledgements</b>	<b>39</b>
<b>Bibliography</b>	<b>40</b>

# Acronyms

Cb: Cumulonimbus

FMI: Finnish Meteorological Institute

TCU: Towering cumulus

METAR: METeorological Aerodrome Report

CIN: convective inhibition

CAPE: convective available potential energy

LFC: level of free convection

EL: equilibrium level

ICAO: International Civil Aviation Organization

ARP: aerodrome reference point

PRF: pulse repetition frequency

FAR: False Alarm Ratio

POD: Probability of Detection

CSI: Critical Success Index

# 1. Introduction

Cumulonimbus (Cb) clouds are a serious threat to aviation as they can produce hazardous weather such as turbulence, icing, lightning, wind shears, micro-bursts, hail and intense precipitation (International Civil Aviation Organization, 2018). These severe weather hazards associated with Cb clouds increase the annual costs of the aviation industry due to the increased time and lost fuel, as some flights might be delayed, cancelled or rerouted. For all of the above reasons, it is important to forecast, detect and monitor Cb clouds as well as possible. Therefore, it is also relevant to understand convection since it initiates Cb clouds.

Finnish Meteorological Institute (FMI) is responsible for providing aeronautical meteorological services in Finland (Finnish Meteorological Institute, 2020b). This includes doing the METeorological Aerodrome Report (METAR), which describes the weather at the aerodrome and its vicinity. At Helsinki-Vantaa airport (EFHK) METARs are done by a human observer around the clock all year round. At all other Finnish airports, METARs are at least partially done automatically. Automatic METAR is called AUTO METAR. Since significant weather is reported in METAR, also towering cumulus and Cb clouds must be included. On METARs done manually by an observer, Cb detection is primarily based on the observer's observations on the shape and the height of the cloud (Nikkanen, 2020). Sometimes, Cb detection conditions can be more difficult, for example, when it is dark or if the Cb cloud is embedded in the cloud layer. In addition, having human observers working around the clock all year around is costly. Therefore, automation of Cb detection is a topical matter.

Also other countries are interested in automatic Cb detection in Europe. For example, a system that is using both radar and satellite observations is used in the Netherlands (De Valk & van Westrhenen, 2015). In addition, a similar system is applied in Germany (Kober & Tafferner, 2009). According to Honoré et al. (2010), France operates a system that uses lightning and weather radar observations to detect Cb clouds. Automated Cb detection systems are not only used in Europe but around the world. For example, they are nowadays applied at some airports in Japan (Japan

Meteorological Agency, 2016) and in New Zealand (Hartley & Quayle, 2014).

FMI is likewise applying an algorithm that uses observations from weather radars to detect Cb clouds (Hyvärinen et al., 2015). Information of Cb clouds has been in AUTO METARs from years 2018-2019 (Nikkanen, 2020). Also, human observers can utilise it when detecting Cb clouds. It is reasonable to study how well this scheme can detect Cb clouds and what could be done to improve it. The operation of the algorithm is based on the ability of the weather radar to detect precipitation. Precipitation is detected with a value called a radar reflectivity factor.

The aim of this thesis is to examine how well FMI's algorithm can detect Cb clouds compared to manual observations. Summer months are studied as Cb clouds are more common and stronger in Finland than due to more unstable atmosphere (Eastman & Warren, 2014). The reasons for differences are discussed, and furthermore, improvements for the algorithm are suggested. A hypothesis is that the weather radar observations and the algorithm, when it is working properly, could be better than human observations in most cases. Therefore, the algorithm could be the only tool that is used to detect Cb clouds for both manual and automatic METARs in the future.

In the next chapter, Chapter 2, some theory and background information, which helps to understand the later study, will be discussed. Then, Cb clouds and METARs are explained in more detail. In addition, the basics of radar meteorology and radar geometry are considered.

After the theory chapter, data and methods used in this thesis are described in Chapter 3. In the following Chapter 4, the results of this thesis are processed and reviewed. Furthermore, some case examples are introduced to deepen understanding of differences and similarities between human observation and algorithm detection. Also, possible future steps are introduced and discussed. Finally, conclusions are drawn in Chapter 5.

## 2. Theory

### 2.1. Convection

Convection is transport of heat, momentum and moisture due to the movement of fluid in the atmosphere. Conceptually, convection transfers warm air upward and cold air downward. Heat can be either sensible or latent. Latent heat is related to a substance changing its physical state, for example, when water vapour is condensed into liquid water droplets. If no clouds are formed by convection, the convection is called dry. When phase changes of water have an essential role in convection and clouds are formed, the convection is called moist (Emanuel, 1997). Nevertheless, both types of convection remove excessive heat from the surface and transport it into the atmosphere. When the vertical motions extend from the lower atmosphere above 500 hPa, convection is referred to as deep (Davidson, 1999). So before discussing Cumulonimbus (Cb) clouds, it is important to understand deep moist convection, which is responsible for Cb and other cumulus cloud development (Markowski & Richardson, 2010). In this thesis, deep moist convection is referred to as convection.

Two requirements need to be fulfilled so that convection can initiate (Markowski & Richardson, 2010). The first one is that air needs to reach its level of free convection (LFC). This typically means that air needs some forced ascent to get there since some amount of convective inhibition (CIN) is usually present. CIN is the amount of energy that will prevent an air parcel from rising from the surface to LFC (Markowski & Richardson, 2010). It can be written as

$$CIN = - \int_0^{LFC} B dz \quad (2.1)$$

where  $B$  is the buoyancy force.  $B$  is integrated from the surface to the LFC. CIN is negative because it is the work that must be done to lift an air parcel to LFC.

From LFC, an air parcel can freely accelerate upward as it becomes buoyant relative to its environment (Holton & Hakim, 2012). The second requirement is that the air

parcel should have convective available potential energy (CAPE), which means that after reaching LFC, the air parcel must remain positively buoyant in a deep enough layer. CAPE can be written as

$$CAPE = \int_{LFC}^{EL} B dz \quad (2.2)$$

where  $B$  is the buoyancy force.  $B$  is integrated from LFC to the equilibrium level (EL). At the EL, the air parcel has become equal to the temperature of the surrounding air. Above the EL, the air parcel becomes negatively buoyant and convection stops. However, the air parcel might continue to rise after EL because it still has some kinetic energy left at EL. The Equation 2.2 tells that CAPE is equal to the amount of work done by the buoyancy force. Figure 2.1 below illustrates an example of a sounding. CIN, CAPE, LFC and EL are also marked in Figure 2.1 where the light blue area is CIN, and the orange area is CAPE.

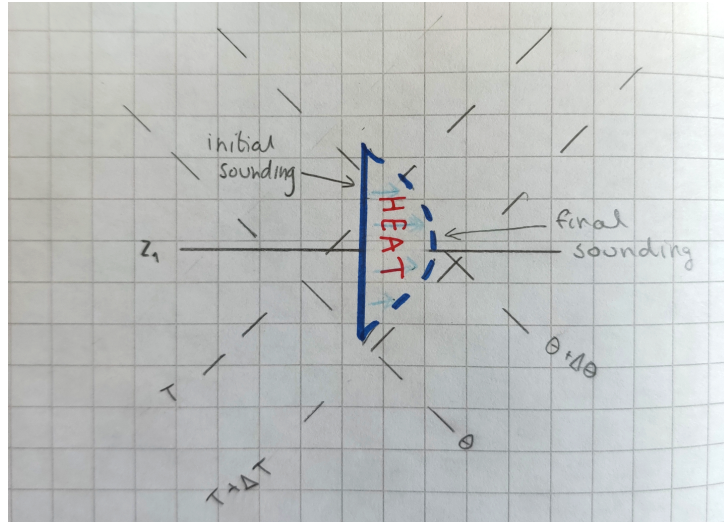


**Figure 2.1:** Example of a sounding. CIN = light blue area, CAPE = orange area. LFC (as  $LFC_T$ ) and EL are marked in the figure.

Since large CAPE values are needed for convection to initiate, conditions when it happens need to be understood. Large CAPE values are possible when temperature lapse rate in lower and middle troposphere is at least larger than moist adiabatic lapse rate  $\Gamma_s$  (Markowski & Richardson, 2010). That way lifted air parcel will cool down slower than its environment. Temperature lapse rate is large when the boundary layer is warm and moist and the free troposphere is cold. The lapse rate tendency equation 2.3 tells how the temperature lapse rate can change and thus initiate convection:

$$\frac{\partial \gamma}{\partial t} = \underbrace{-\mathbf{v}_h \cdot \nabla_h \gamma}_I - \underbrace{w \frac{\partial \gamma}{\partial z}}_{II} + \underbrace{\frac{\partial \mathbf{v}_h}{\partial z} \cdot \nabla_h T}_{III} + \underbrace{\frac{\partial w}{\partial z} (\Gamma_d - \gamma)}_{IV} - \underbrace{\frac{1}{c_p} \frac{\partial q}{\partial z}}_V. \quad (2.3)$$



Term I represents horizontal and term II vertical lapse rate advection. Term III is differential temperature advection when it is combined with the first term. Term IV is called a stretching term. The last term V is diabatic heating.  $\mathbf{v}_h$  is the horizontal wind velocity,  $w$  is the vertical wind velocity,  $\Gamma_d$  is the dry adiabatic lapse rate,  $c_p$  is the specific heat at constant pressure and  $q$  heating rate. The derivation of the above Equation 2.3 is not shown in this thesis since it is unnecessary. It is here only to show what factors have an effect on lapse rate tendency.

Next, a simple example of how lapse rate can change to initiate convection is presented. In this example, term V from Equation 2.3 is changed to modify lapse rate. When diabatic heating is decreased with height, it means that the differential  $\frac{\partial q}{\partial z}$  is negative. Since the specific heat at constant pressure  $c_p$  is a positive constant, the lapse rate is increased in time ( $\frac{\partial \gamma}{\partial t} > 0$ ). Similarly, when diabatic heating is increased with height, the lapse rate is decreased. This example is shown in Figure 2.2, where above the maximum heating level ( $z_1$ ) lapse rate is increased and below decreased.

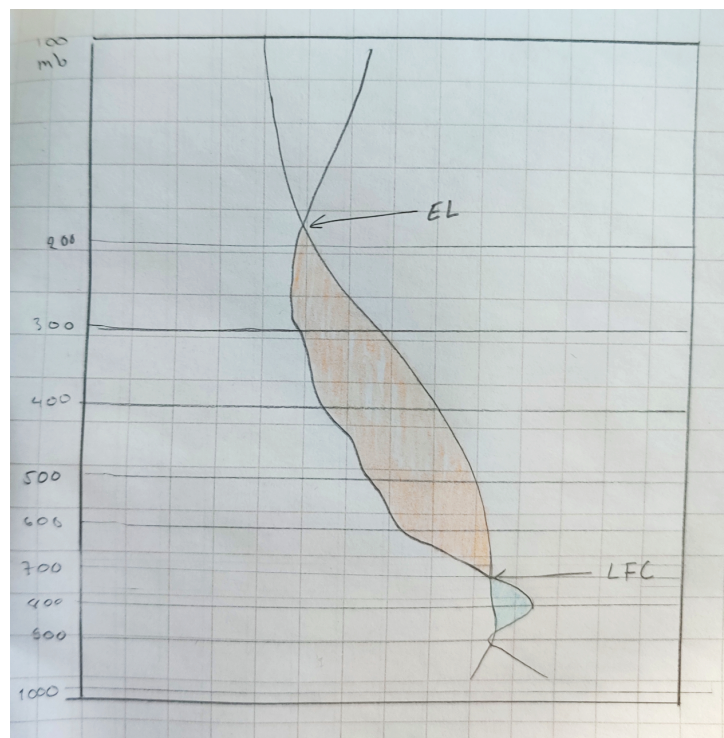


**Figure 2.2:** Example of how differential diabatic heating can change lapse rate.

There are also other ways that can change CAPE and CIN without changing the lapse rate. For example, CIN can be reduced by low-level moistening or warming (Markowski & Richardson, 2010). Especially low-level moistening is independent of lapse rate changes. Low-level warming and deepening of the low-level atmosphere are common when the Sun

is rising. That leads to decreased CIN, which makes convection initiation easier. Note that both low-level warming and moistening also have a positive effect on CAPE. Another way to change CIN and CAPE without changing lapse rate is through a large scale ascent (Markowski & Richardson, 2010). That is because the mean ascent is associated with adiabatic cooling that leads to reduced CIN.

## 2.2. Cumulonimbus cloud

Clouds can be classified according to their shape and height. There are three different classes for the height classification: the bases of the low-level clouds are from 0 to 2 km, the bases of the middle-level clouds are from 2 to 7 km, and the bases of the high-level clouds are from 5 to 13 km (Karttunen et al., 2001). Cumulonimbus<sup>1</sup> (Cb) clouds are classified as low-level clouds, yet they can still extend to all three height levels (Karttunen et al., 2001).

According to World Meteorological Organization (2017), a Cb cloud is an optically dense cloud with a significant vertical extent, which is approximately ten kilometres, and it is formed by convection. Its upper part is almost always flattened, it spreads out like an anvil and is usually smoothed, fibrous or striated. The base of the cloud is often dark, and there are usually low, ragged clouds. Picture 2.3 below is a good example of a Cb cloud.



**Figure 2.3:** Cumulonimbus cloud. (World Meteorological Organization, 2017)

There is always rain in a Cb cloud, and the rain is of showery type. A Cb cloud can also produce lightning, thunder and hail. A Cb cloud can initiate from different cloud types, i.e. from Cumulus congestus, Altopcumulus castellanus, Stratocumulus castellanus, or it can also be embedded in Altostratus or Nimbostratus (World Meteorological Organiza-

---

<sup>1</sup>*Cumulus* is a Latin word meaning heaped and *nimbus* rainstorm.

tion, 2017). Because a Cb cloud forms most commonly from Cumulus congestus, it is sometimes difficult to distinguish them. The cloud is identified as Cb when its upper part loses its sharpness or presents a fibrous or striated texture (World Meteorological Organization, 2017).

Cb clouds can be isolated, appear in clusters or along fronts. Duration of one single cell is usually about 0.5 – 2 hours, and the diameter can be from 500 metres up to 20 kilometres (Karttunen et al., 2001). Single-cell convection is next considered. There are three different stages of a storm in single-cell convection: towering cumulus stage, mature stage and dissipating stage. These different stages are illustrated in Figure 2.4. Towering cumulus stage is a stage where there is only an updraft, and the lifecycle of an ordinary cell begins with this stage. The anvil starts to form in the mature stage, and the water droplets in this stage are large enough to fall through the updraft. The falling precipitation and the evaporation of precipitation induce a downdraft. The gust front at the ground is formed to the leading edge of the downdraft. There is heavy precipitation and, additionally, lightning is possible in the mature stage. The dissipating stage begins when the downdraft dominates the cell, and the updraft cannot be maintained. Now, new cells can be initiated by the gust front. Initiation depends on CIN and vertical motions in the gust front. Figure 2.4 visualises the three different stages in single-cell convection.

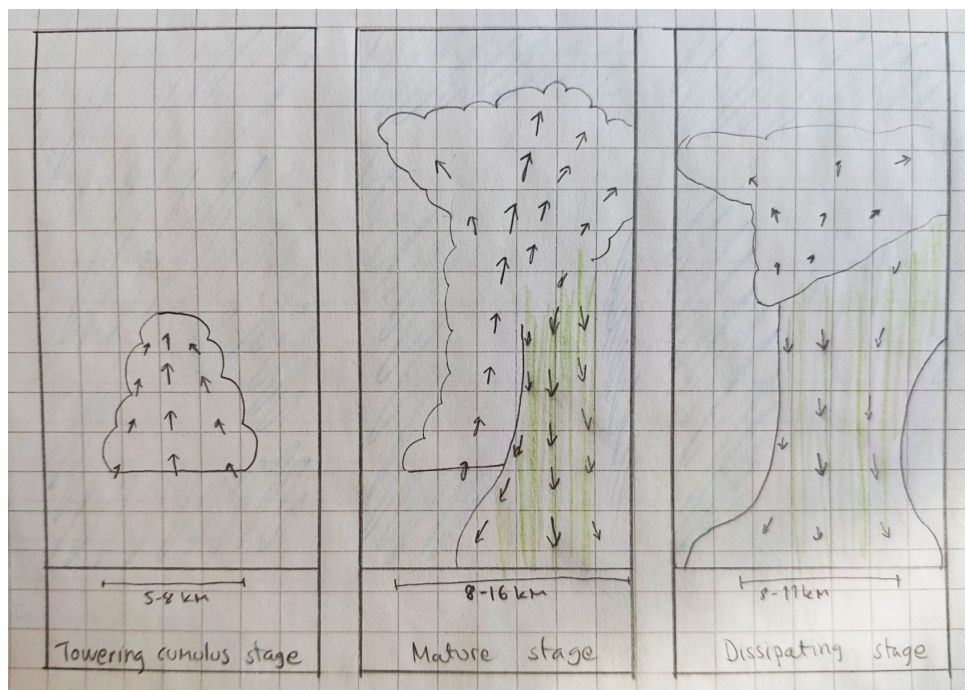


**Figure 2.4:** Schematic figure of three stages of an ordinary convective cell.

Multicellular convection consists of multiple single-cells where each cell is in the different

stage, and the new single-cells are repeatedly generated by the gust front (Markowski & Richardson, 2010). Multicellular convection is the most common type of convection in the mid-latitudes. If the circumstances in the atmosphere are favourable, supercellular convection may be initiated. Supercells can last up to 9 hours but are very rare in Finland, so they are not studied in detail (Karttunen et al., 2001).

Cb clouds appear in Finland mostly in summer when unstable lower troposphere is more common than in winter (Karttunen et al., 2001). That is why a dataset from the summer months is used in this thesis. However, they can still form in winter, for example, over the Gulf of Finland if the sea surface is unfrozen. Vertical extent of cb clouds in winter is lower as the troposphere is colder, more stable and the tropopause is lower (Karttunen et al., 2001).

### 2.3. METAR

Finnish Meteorological Institute (FMI) is responsible for providing aeronautical meteorological services for civil and military users in Finland (Finnish Meteorological Institute, 2020b). METeorological Aerodrome Report (METAR) is one of the services that FMI provides. METAR is a local routine observation report that describes the weather at the aerodrome or its vicinity (International Civil Aviation Organization, 2018).

METARs are regulated by the International Civil Aviation Organization (ICAO) and EU. ICAO and EU define the content, format and release time of the METARs (International Civil Aviation Organization, 2018). ICAO regulates that METAR report must contain the following information:

- location indicator
- observation time
- surface wind direction and speed
- visibility
- runway visual range (when applicable)
- present weather
- cloud amount
- cloud type (only if the cloud is towering cumulus (TCU) or cumulonimbus type)
- height of the cloud base (or vertical visibility where measured)
- air temperature
- dew-point temperature
- the atmospheric pressure (QNH/QFE).

METARs are primarily used by aircraft pilots who use it for the flight planning and meteorologists who use it for the weather forecasting among other products.

In Finland METAR observations are done every 20 and 50 minutes past the hour. Only the operationally significant weather is reported in METAR, and according to the ICAO regulations, clouds and other remarkable weather phenomena are observed within a maximum radius of 16 kilometres from the aerodrome reference point (ARP) (International Civil Aviation Organization, 2018). ARP is the geographical location of an aerodrome. METARs can be done manually by human or automatically. If the METAR is done automatically, it is specified in the head of the METAR after the time group with the word AUTO. Helsinki-Vantaa airport is the only airport in Finland where METARs are done by a human observer around the clock all year round.

Clouds at the aerodrome or its vicinity (maximum radius of 16 km from the ARP) are reported in METAR if they are operationally significant (International Civil Aviation Organization, 2018). This means that clouds with a base under 1500 metres (5000 feet) or TCU or Cb clouds are reported. In reality, a human observer observes significant clouds over the 16 kilometres radius (Isolähteenmäki, 2020). Usually, this happens if the observer thinks that it is important to air traffic: for instance, if Cb cloud is near the runway. An observer can identify Cb cloud based on the shape and height of the cloud. This information is discussed in the previous section in more detail, but the cloud can be identified as Cb if its vertical extent is large, the upper part of the cloud spreads out like an anvil, and the outline of the cloud top is not as sharp as in a TCU. In addition, if the cloud base is very dark, the cloud is usually identified as Cb, even if the cloud is embedded in the cloud layer, and the cloud top is not visible (Tikkamäki, 2020). A clear indication of Cb cloud is thunder, lightning or both. Also, if the precipitation is of a showery type or in the form of virga, it can be classified as Cb cloud.

Cb clouds can be identified manually with the help of ceilometers. Ceilometers determine the height of a cloud base by using a laser or other light source. There are several ceilometers at Helsinki-Vantaa, which are used especially when determining the height of the cloud base or vertical visibility (Finnish Meteorological Institute, 2020b). In addition, an observer can use radar observations to determine whether the cloud is Cb.

In some cases, manual Cb detection can be better than automatic detection since the observer is often aware of the meteorological situation and can utilise his/her expertise to detect the Cb cloud even when it is not visible (International Civil Aviation

Organization, 2018). On the other hand, the manual Cb detection can be difficult if it is dark or when the Cb cloud is buried in clouds and the cloud tops are not visible (EMBD CB situation). For example, Cb clouds can be obscured by other low clouds in a frontal system. In these cases, the automatic Cb detection algorithm can be better than human. In addition, also other reasons support automatic Cb detection; measurements are objective and it also saves money not to have staff working in shifts. Therefore, the automatic algorithm that can detect Cb clouds with a sufficient accuracy could be the choice of the future in Finland. Later in this thesis, it is studied how accurately the algorithm detected Cb clouds compared to the manual observations in the summers of 2016-2020.

## 2.4. Weather radar geometry

Radars are used in a wide variety of applications. In this section, the focus is on weather radars that can be used to observe the atmosphere. The weather radars operate in microwave frequency range since the microwaves can reveal the inner structure of intense storms and Cb clouds (Rauber & Nesbitt, 2018). This is a major advantage of radar Cb detection because an observer cannot see the inner structure of a cloud. Radars at FMI have a wavelength of 5.3 centimetres which means these are C-band radars (Saltikoff et al., 2010).

The antenna of the weather radar sends high powered microwave pulses in different directions. When the pulse encounters a target, part of its power is reflected and scattered back to the antenna (Rauber & Nesbitt, 2018). Subsequently, the weather radar receiver measures the power of the reflected pulse and its travel time. The former tells the intensity of precipitation, and the latter tells the distance of the obstacle from the radar. The more intense precipitation, the stronger the echo is. Weather radars cannot detect convective clouds before water vapour is condensed into liquid water droplets. They are very sensitive devices, as the power of the reflected pulse is only a tiny fraction of the total transmitted power. To illustrate this, the transmitted power can typically be 250 000 watts, and the reflected power can be only from  $1 \cdot 10^{-6}$  to  $1 \cdot 10^{-7}$  watts.

FMI's weather radar in Vantaa, Kaivoksela is used in this thesis because it is close to Helsinki-Vantaa airport where METARs are reported. Technically, the data is from a composite that covers the whole Finland, but as the radar in Vantaa is closest to Helsinki-Vantaa airport, and there are no other radars in the vicinity, the radar in Vantaa is the one which has taken the measurements needed in this thesis. The model of the radar is WRM200, and it is manufactured by Vaisala. WRM200 is a dual-polarization

Doppler radar. In order to understand the Cb detection algorithm, it is essential to understand the basics of radar measurement geometry. Measurements on a daily basis are carried out as elevation scans. This means that with each scan the circular antenna rotates 360 degrees with a constant elevation angle. From this, one conical surface is produced. The measurements consist of several elevation scans which produce a set of nesting conical surfaces. This dataset is called a volume scan. A volume scan is done every five minutes, although the specific elevation angles used in a volume scan vary slightly depending on the time (Finnish Meteorological Institute, 2020c). For instance, hh:00-hh:05 scan uses 13 different elevation angles, whereas hh:05-hh:10 scan uses nine different elevation angles. In Figure 2.5 below, the volume scan is illustrated.

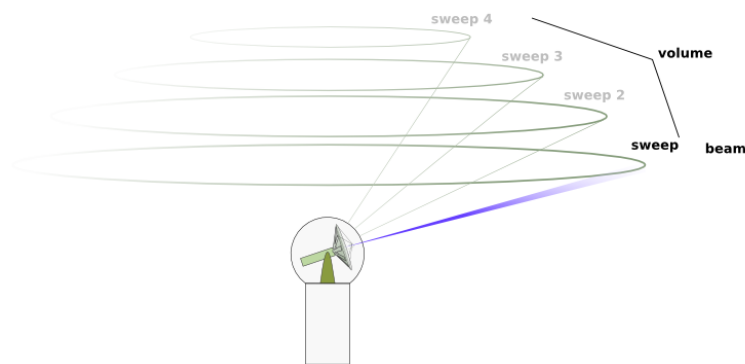


**Figure 2.5:** Volume scan. Figure by Markus Peura.

Cb detection with the weather radar is based on the quantity called a radar reflectivity factor  $Z(\text{dBZ})$  which is called as a radar reflectivity in common usage (Rauber & Nesbitt, 2018). The radar reflectivity factor is probably the most important quantity in radar meteorology. The radar reflectivity factor is related to the power that is returned back to the weather radar by the weather radar equation. It can be calculated as

$$Z = \frac{\sum_j D_j^6}{V_c} \quad (2.4)$$

where  $D$  is a diameter of hydrometeor and  $V_c$  is a unit volume. Subscript  $j$  represents that summation is carried out over all scattering targets. Note, that in this Equation 2.4, it is assumed that the Rayleigh assumption is valid. This means that hydrometeors are small compared to the wavelength of the radar (Rauber & Nesbitt, 2018). With a C-band radar, this assumption is not valid if the size of hydrometeor is larger than approximately 2 centimetres which means that the type of the hydrometeor is hail. In addition, hydrometeors must be spherical. This condition is only met by small raindrops, some frozen raindrops and some graupel and hail (Rauber & Nesbitt, 2018). However, Rayleigh scattering is usually assumed, although it is unlikely to be met in many cases.



When it is obvious that the Rayleigh criteria cannot be assumed, the term equivalent radar reflectivity factor can be used (Rauber & Nesbitt, 2018). In this thesis, it is not discussed in more detail because it is irrelevant for the basics of the radar measurements. Although the radar receives power that was scattered back to radar, it does not tell anything alone. In practice, the radar reflectivity factor is needed since a parameter that is more directly linked to the physical properties of the precipitation is wanted. When the reflectivity factor is of a certain size, the target can be classified as a Cb.

The algorithm which FMI is using is adopted from Météo-France (Leroy, 2006). Radar takes measurements every five minutes, which means the Cb cloud analysis is done equally often. It is done by investigating the vertical structure of reflectivities from radial resolution data (Hohti, 2020). In the beginning, individual points and radial lines that are considered as clutter are cleaned from the polar data. It is then investigated if the reflectivity threshold values are exceeded in a sufficient number of different heights. According to Leroy (2006), France is using the following reflectivity threshold values for Cb: lower threshold value is 33 dBZ, and the upper one is 41 dBZ. In addition to the definition by Leroy (2006), there are some additional criteria at FMI that need to be fulfilled for the reflection to be classified as a Cb cloud (Hohti, 2020):

- these threshold values are implemented to a vertical column of a polar volume
- the reflectivity factor should exceed the lower threshold value for at least in two elevation angles
- the reflectivity factor should exceed the upper threshold value at least in one elevation angle
- these threshold values are decreased a few dBZ as a function of distance, as smoothing of small phenomena increases when the distance from the radar increases
- the reflectivity must be consistent in a vertical direction: gaps, where the radar reflectivity factor drops below 5 dBZ, are not allowed
- to avoid ground clutter, measurements are accepted approximately only above 200 metres.

When all the aforementioned conditions are met, the target is classified as Cb. A graphical explanation of what the reflection could look like when a weather radar observes Cb is in Figure 2.6 below.



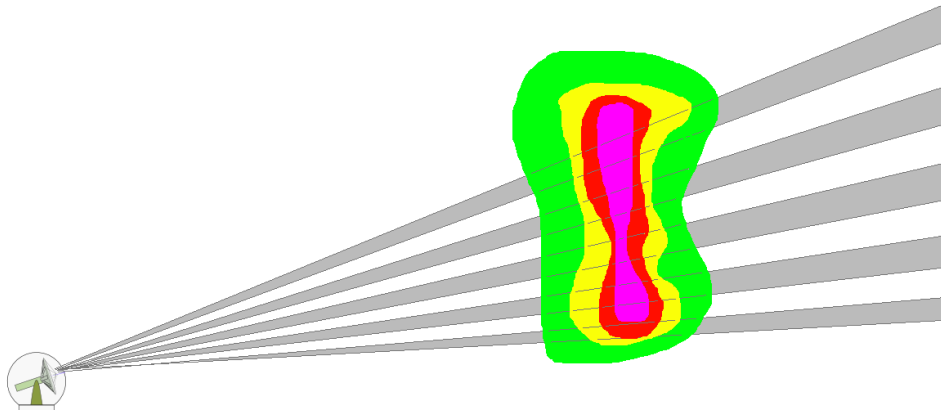


**Figure 2.6:** Example of Cb observed by radar. Colours describe the reflectivity factor. Red:  $33 \text{ dBZ} < Z < 41 \text{ dBZ}$ . Purple:  $Z > 41 \text{ dBZ}$ .

Next, a real vertical cross-section of Cb and the related radar reflectivity factor is introduced. This is illustrated in Figure 2.7, which is a pseudo-range-height indicator (pseudo-RHI) image. This means that the image is interpolated from a 3D volume consisting of several azimuthal scans. It can be seen that the radar reflectivity factor is at its greatest about  $44 \text{ dBZ}$  in the middle of a Cb cloud. This fulfils the upper threshold value ( $Z > 41 \text{ dBZ}$ ) at least in one elevation angle. The lower threshold value ( $Z > 33 \text{ dBZ}$ ) is also fulfilled at least in two elevation angles. Thus, the reflection in Figure 2.7 is clearly classified as a Cb.

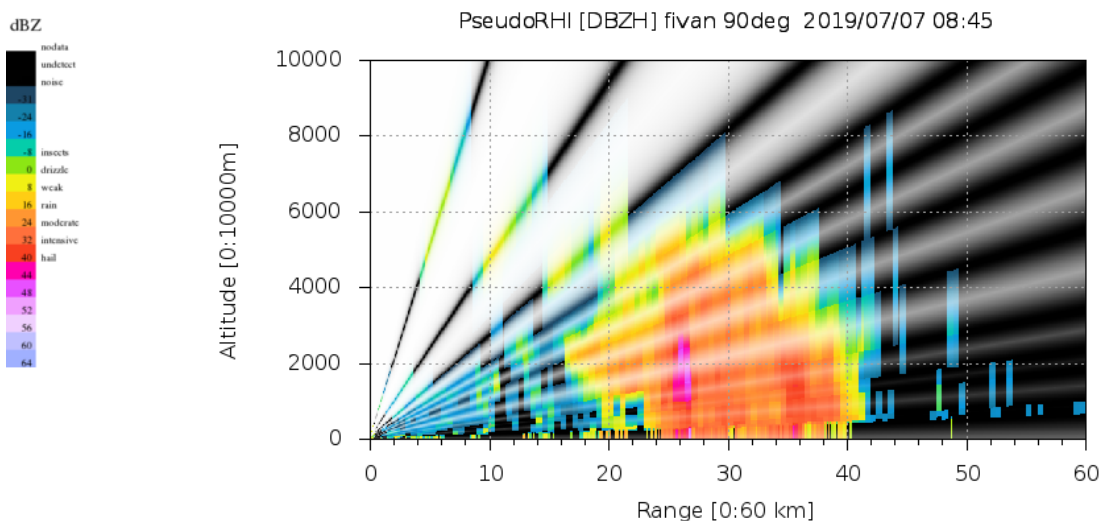


**Figure 2.7:** Pseudo-RHI image of Cb.

This situation in Figure 2.7 can be seen in Figure 2.8 as a plan position indicator (PPI) image. The pseudo-RHI image in Figure 2.7 is a cross-section to the east from the Vantaa radar. The small black cross in Figure 2.8 represents approximately the location of the radar.

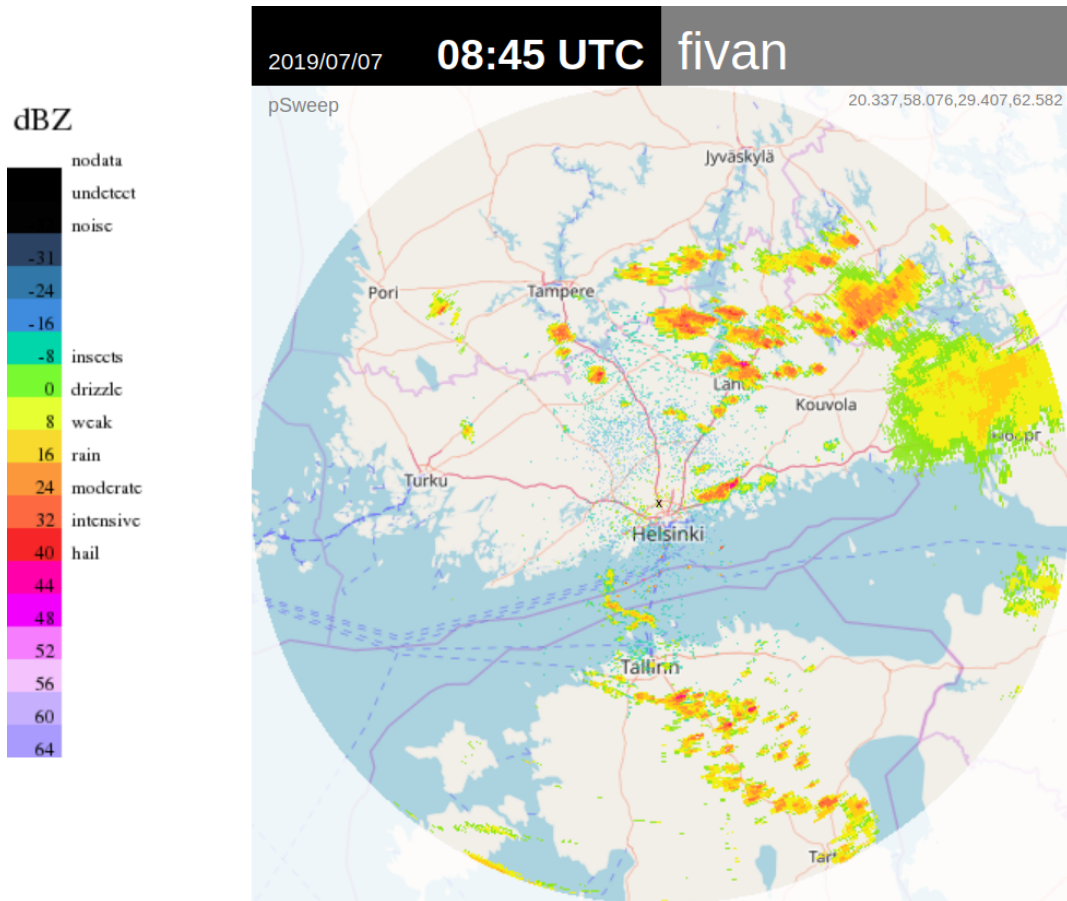


**Figure 2.8:** PPI image of Cb.

Since the weather radars at FMI are dual-polarization radars, their measurements contain some additional variables. That is due to dual-polarization radars transmit and receive pulses in both vertical and horizontal direction (Rauber & Nesbitt, 2018). As a result, they give more information about the size and shape of the targets. For instance, one of these variables is called differential reflectivity  $Z_{DR}$  (Rauber & Nesbitt, 2018). Differential reflectivity is the difference between horizontal reflectivity and vertical reflectivity:  $Z_{DR} = Z_H - Z_V$  and it can help to identify hydrometeors (Woodard et al., 2012). Also, two other variables, the correlation coefficient  $\rho_{HV}$  and the specific differential phase  $K_{DP}$  can be used in identifying hydrometeors. The identification of hydrometeors is important since the type of hydrometeor can tell about the presence of Cb clouds. For instance, supercooled raindrops above the freezing level have predicted lightning to occur (Woodard et al., 2012).

Effective measurement range of the radar depends on the weather. Theoretically, with the setup used at FMI, the measurement range of the weather radar can be up to

250 kilometres. This maximum range is defined as

$$r_{max} = \frac{c}{2(PRF)} \quad (2.5)$$

where  $c$  is the speed of light and PRF is the pulse repetition frequency (Rauber & Nesbitt, 2018). PRF depends on the type of radar, but it is usually 100-1000 times in a second. Targets that radar is observing must be within  $r_{max}$ . The PRF is approximately 570 per second at FMI (Saltikoff et al., 2010), so  $r_{max}$  can be calculated as

$$r_{max} = \frac{299792458m/s}{2 * 570Hz} = 262975.84035...m \approx 250km. \quad (2.6)$$

However, e.g. snowfall in winter can be detected with a maximum range of 120 kilometres. One reason for this is that clouds are lower in winter and therefore below the radar beam (Karttunen et al., 2001). In addition, the curvature of the earth limits echoes of targets to be within  $r_{max}$ : if a target is beyond  $r_{max}$ , it is likely to be below the radar beam and radar cannot detect it (Rauber & Nesbitt, 2018).

### 3. Data and methods

This chapter discusses in more detail the data used and how it is processed in this thesis. In addition, different kinds of verification scores are introduced.

A dataset that contains the summer months from 2016 to 2020 is used in this thesis. June, July and August are considered as summer months. The radar dataset is compared with METARs since it is considered that METARs give the best information about the presence of Cb clouds at Helsinki-Vantaa airport and its vicinity. METARs are sent every 20 and 50 minutes past the hour, and the observation time for the METAR is ten minutes before it needs to be sent (Finnish Meteorological Institute, 2020a). Weather radars make one full volume scan every 5 minutes in Finland. Because the METARs and the radar measurements have a different schedule, they need to be matched together. There are two ways this can be done. The first option is to use the radar data from 20 and 50 minutes past the hour because that time is as close as possible with the time that METAR needs to be sent. The second option is to use the radar data from both 15 and 20 minutes past the hour and 45 and 50 minutes past the hour to cover the whole ten-minute METAR observation period. Both options are considered and compared, which one of the methods would be better in this thesis.

After pairing these two observation sources, differences between the Cb detection algorithm and human-based METAR observations are analysed. In total, the dataset contains 22048 METAR observations. This means there are 32 METARs missing since theoretically there should be 22080 METARs from that specific time period. From the 22048 METARs, there are 2266 METARs where Cb was observed, and 19782 METARs where Cb was not observed. Furthermore, it is studied how many cases there are where both the algorithm and human observations did not detect a Cb cloud. Various dichotomous verification scores are calculated for the radar-METAR Cb observation-pairs. Finally, it is discussed what caused the disagreements between detection of the algorithm and observer's observations.

After the whole dataset is studied, it is divided into two groups: one for daytime

observations and the other one for night-time observations. The daytime is specified to be between 6 UTC – 18 UTC, and the night-time between 18 UTC – 6 UTC as the same hours are used in some SYNOP measurements. Note, that in summer there is dark approximately only five to nine hours per night. The difference between the night-time and daytime Cb detection accuracy is studied.

Then, it is studied if there are any differences in the detection accuracy between different years or months. First, different verification scores are calculated individually to each year and compared together. After that, the dataset is grouped by month, and similarly what was done to different years, verification scores are calculated to each month and compared with each other.

It was mentioned before in Chapter 2 that the range of weather radars can be even 250 kilometres in good weather. In the algorithm, such long range is not necessary since ICAO standards regulate that Cb clouds have to be detected at the aerodrome and its vicinity (International Civil Aviation Organization, 2018). Therefore, the range in the Cb detection algorithm is specified to be 20 kilometres. Similarly, the observer at the airport is only detecting Cb clouds in the range of approximately 16 kilometres. The algorithm uses a larger range because sometimes the observer’s detection range can be a bit over 16 kilometres. The radar in Vantaa is close to Helsinki-Vantaa airport.

A starting point to Cb detection with weather radars is the polar data (ODIM HDF5 format) (Finnish Meteorological Institute, 2020c). The algorithm was described in more detail in Chapter 2, so it is not repeated here. The detection algorithm has been pre-operative at FMI since 2011 and meteorologists have been using it among other tools, especially under challenging conditions. These difficult conditions include darkness or embedded Cb, for example.

### 3.1. Validation

Cb cloud detection can be regarded as a dichotomous event, and therefore it can be referred to as yes/no events. The possible outcomes can be presented in a contingency table where all the possible outcomes of an event are shown (Jolliffe & Stephenson, 2012). In this study, the contingency table has a shape of 2x2. The contingency Table 3.1 can be used to determine numerous verification scores (Wilks, 2011).

Different verification scores can tell about the accuracies of the results, and they can be calculated from the number of hits, false alarms, misses and correct negatives.

Hits are the cases when both the algorithm and the observer detected a Cb cloud. Misses mean the cases where the observer detected a Cb cloud, but the algorithm did not. On the contrary, false alarms mean the cases where the algorithm detected a Cb cloud, but the observer did not. Note, it does not necessarily mean that the algorithm was wrong: it can also be a case when the observer could not see a Cb cloud. However, human-based observations are used as the ground truth in this study, so that is why these kinds of cases are called false alarms. Correct negatives are the cases when both the algorithm and the observer did not detect a Cb cloud. Not all scores mentioned below are used to measure the accuracy but some other value, for instance, over- or underdetecting of Cb clouds.

	Observed 1	Observed 0
Detected 1	Hits	False alarms
Detected 0	Misses	Correct negatives

**Table 3.1:** A contingency table. (Wilks, 2011)

From the contingency table 3.1, several different verification scores can be calculated. In this thesis, the False Alarm Ratio (FAR), the Probability of Detection (POD), the Critical Success Index (CSI) and the bias are used to analyse the results.

The FAR is the fraction of the detections where a yes-event was detected but not observed (Wilks, 2011). False Alarm Ratio is calculated instead of False Alarm Rate ( $\frac{False\ alarms}{False\ alarms + Correct\ negatives}$ ) because the occurrence of Cb clouds is a rare event and thus False Alarm Rate could become misleadingly low when the number of correct negatives is high. In this thesis, an observed yes-event is an event when an observer observed a Cb cloud. Likewise, a detected yes-event is an event when the algorithm detected a Cb cloud. So, FAR is the fraction of the cases when the algorithm detected a Cb cloud but the observer did not. The FAR can have values from 0 to 1. The smaller the FAR is, the better Cb detection with the algorithm is. In other words, if the FAR is 0, the detection was always also observed. FAR tells about the reliability of the scores. FAR can be calculated as the following:

$$FAR = \frac{False\ alarms}{Hits + False\ alarms}.$$

The POD is the ratio of observations where yes-event was both detected and observed to the number of detections where yes-event was both observed and detected (hits) or only observed (misses) (Wilks, 2011). In this study, it means that POD is the cases where both the algorithm and the observer observed a Cb cloud divided by the number of times a Cb cloud was observed. The POD can have values from 0 to 1, but unlike with FAR, 1

is the best score for the POD. POD can be calculated as:

$$POD = \frac{Hits}{Hits + Misses}.$$

The CSI (also called as the threat score) is the correct forecasts (hits) divided by the total number of detections where yes-event was detected, observed or both (Wilks, 2011). It can have values from 0 to 1. The bigger the CSI value is, the more accurate Cb detection with the algorithm is. CSI describes the accuracy well with low-frequency events since the correct negatives are not considered (Jolliffe & Stephenson, 2012). Cb clouds can be considered as rare events according to the numbers in the contingency table. According to Jolliffe & Stephenson (2012), CSI would not be suitable even for rare events because it tends to a limit of zero when observed events are close to zero. However, this is not the case in this study, so CSI can be used. CSI can be calculated as the following:

$$CSI = \frac{Hits}{Hits + Misses + False\ alarms}.$$

The bias is a ratio of the number of detections to the number of observations (Wilks, 2011). In this thesis, it means that it is a ratio between the detected Cb clouds by the algorithm and the observed Cb clouds by the observer. If bias is equal to one, it means that the number of times the event was forecasted and observed were equal. If the bias is under one, it means underdetecting and if it is over one, it means overwarning of the detected yes-events. Bias is not used to analyse the accuracy of the results but to tell if the event is classified more or less than observed. The desired value for bias depends on the user and the event of interest (Jolliffe & Stephenson, 2012). In this study, if the bias were equal to one, Cb clouds were detected as many times as observed. This would be optimal for the study. Bias can be calculated as the following:

$$BIAS = \frac{Hits + False\ alarms}{Hits + Misses}.$$

All in all, FAR and POD tell about the reliability of the detection, but neither one of the measures are suitable on its own (Jolliffe & Stephenson, 2012). As a rule of thumb, the bigger the POD and the smaller the FAR, the better the algorithm is at detecting Cb clouds. However, when FAR is decreased, it yields to decreased POD. Similarly, increased FAR yields to increased POD. In this thesis, POD is prioritised over FAR, which means that increased FAR is accepted as misses and underdetection of Cb clouds are more dangerous to aviation than false alarms and overdetection. CSI tells about the detection accuracy, and it works well with low-frequency events. The bias tells about over- or underforecasting.

## 4. Results

The dataset consists of the summer months from 2016 to 2020. Summer months are defined to be from June to August. The values that are measured 20 and 50 minutes past the hour are chosen from the weather radar data. Next, the METAR dataset is combined with the weather radar dataset and the verification scores are calculated from the combined dataset.

In total, there are 1272 cases where Cb is detected by both human observer and weather radar. There are 994 cases where human observer has detected Cb but weather radar has not. On the contrary, there are 414 cases where weather radar detected Cb but human observer did not. Lastly, there are 19367 cases where neither human observer nor weather radar detected Cb. These aforementioned values are represented in a contingency table in Table 4.1 below.

	Observed 1	Observed 0
Detected 1	1272	414
Detected 0	994	19367

**Table 4.1:** The contingency table of the scores.

Subsequently, FAR, POD, CSI and bias can be calculated from Table 4.1. The theory behind the verification scores can be found in Chapter 3. As a result, the FAR is equal to 0.25, the POD is equal to 0.56, the CSI is 0.47 and the bias is 0.74. Value of bias states that the radar underdetected Cb clouds compared to human observations. This underdetecting is considered to be dangerous to aviation, but it is important to understand that human observers can observe Cb clouds overeagerly and from a bigger radius. Therefore, the result is not as reliable. The POD being 0.56 means that over half of the observed Cb clouds were detected by the algorithm.

The measurements taken 15 and 45 minutes past the hour from the radar data can be included in the calculations. This is done because the observation time for METAR is the past 10 minutes before it needs to be sent. Consequently, the values of 15



and 45 minutes past the hour are taken into account to see if they have any impact on the accuracy of the results. Cb is considered to be detected if there is Cb in either one of the minutes 15 or 20 and 45 or 50 past the hour. The results are represented in Table 4.2.

	Observed 1	Observed 0
Detected 1	1363	515
Detected 0	903	19266

**Table 4.2:** The contingency table of the scores when 15 and 45 minutes past the hour are taken into account.

When the consecutive radar measurements are considered, there are more cases where both the algorithm and observer detected Cb and more cases when only a radar detected Cb. This can be seen from Table 4.2 above. On the other hand, there are fewer cases when only a human observed Cb. FAR, POD, CSI and bias can be calculated from the contingency table 4.2. The FAR is equal to 0.27, the POD is equal to 0.60, the CSI is equal to 0.49 and the bias is equal to 0.83. Compared to the first results, FAR is worse, but POD, CSI and bias are better. As was stated in Chapter 3, increased POD is preferred over decreased FAR; therefore, this result is here considered better than the first one. CSI is also higher, which states that the accuracy of the result is better. The bias is closer to one, which means that underdetecting is not as strong as in the first calculation.

Overall, both the 15 and 20 minutes as well as 45 and 50 minutes past the hour measurements are taken into account in the following calculations since it seems to describe the situation better and give better accuracy of the results. According to Henken et al. (2009), POD is required to be over 0.8 and FAR under 0.2 in order to replace human observers by an automated system in the Netherlands. If these same threshold values were implemented in Finland, the FAR of 0.27 and the POD of 0.60 would not be sufficient enough, and the algorithm as such could not yet replace human observers at Helsinki-Vantaa.

Next, the data are divided into daytime and night-time. The daytime is defined to be from 6 UTC to 18 UTC, and the night-time to be from 18 UTC to 6 UTC. These hours are selected because the SYNOP observations are also done then, and hours from 6 UTC to 18 UTC (local time from 09:00 to 21:00) describe the daytime convection the best. In the daytime dataset, there are total of 1678 METAR observations where Cb was observed, and 9348 METAR observations where Cb was not observed. Likewise, there are 588 METAR observations at the night-time, where Cb was observed, and 10434

METAR observations where Cb was not observed. Then, similarly to what was done to the whole dataset, METAR observations are combined with the radar dataset. The results are illustrated in Table 4.3.

	Daytime	Night-time
Cb was observed by human and radar	996	367
Cb was observed only by human	682	221
Cb was observed only by radar	257	258
Cb was not observed by human or radar	9091	10175
Sum	11026	11021

**Table 4.3:** Values for separate daytime and night-time detections.

It can be seen from Table 4.3 that there is in total almost the same number of observations in both groups, 11026 values for daytime and 11021 values for night-time. However, there are more cases in the daytime when only a human observer has detected Cb and more cases where both the observer and the weather radar have observed a Cb cloud. In general, there are more Cb clouds in the daytime, because the Sun warms the atmosphere and thus destabilizes the boundary layer and initiates convection (Eastman & Warren, 2014).

The diurnal cycle can also be seen in Figure 4.1 below, where Cb observations of each day are summed up and divided into different hours of the day. This is done to both METAR observations as well as radar detections. Figure 4.1 illustrates the same thing that was previously concluded from Table 4.3: there are more Cb clouds in METARs in the daytime and in contrary, more Cb clouds are detected by radar in the night-time. At 06 UTC (09:00 local time), both the radar and human observers observed the same amount of Cb clouds. Note that the hours in Figure 4.1 are UTC (in Finland the time is three hours ahead from UTC). Figure 4.1 shows that most of the Cb clouds are in the daytime, more specifically in the afternoon (highest peaks at 11 UTC, 14:00 local time and 12 UTC, 15:00 local time). In addition, a human observer may prefer to overobserve Cb clouds since it is less dangerous to aviation than underobserving. It is also possible that human observers have observed Cb clouds much further away than 16 kilometres from the ARP since sometimes Cb clouds can appear to be closer than they are in reality (Nikkanen, 2020). In the night-time, overobserving of Cb clouds is more difficult since it is dark.

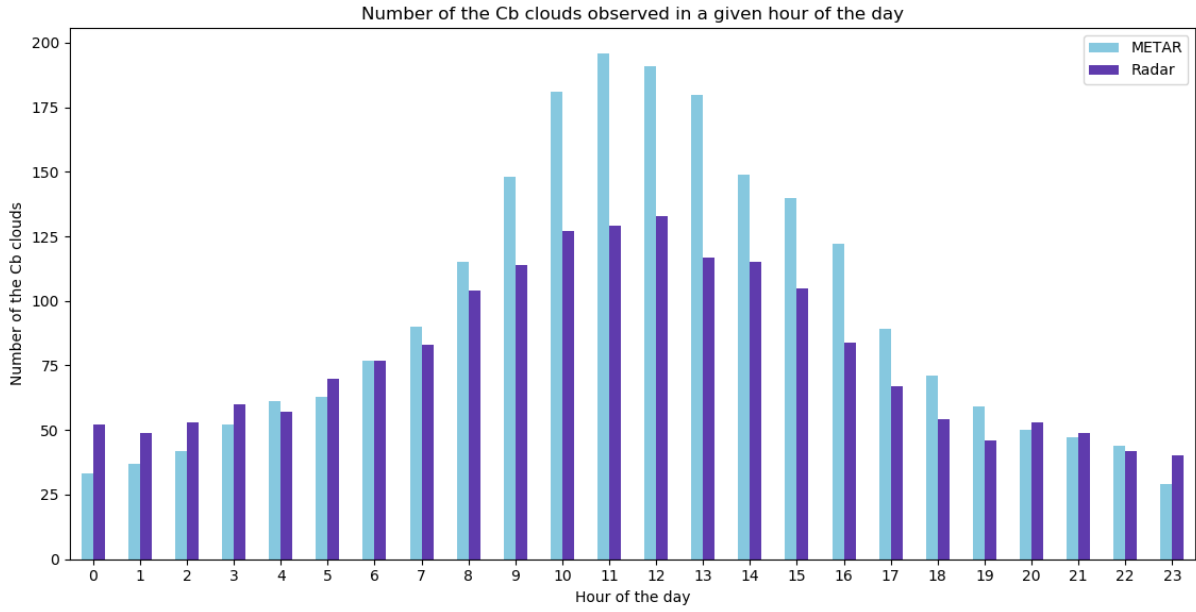


**Figure 4.1:** Cb observations per hour.

Next, the contingency tables can be separately created for both night-time and daytime detections. These values are in Table 4.4.

Daytime			Night-time		
	Observed 1	Observed 0		Observed 1	Observed 0
Detected 1	996	257	Detected 1	367	258
Detected 0	682	9091	Detected 0	221	10175

**Table 4.4:** Contingency tables for daytime (left) and night-time (right) values.

FAR, POD, CSI and bias can be calculated from the contingency tables for daytime and night-time observations, separately. These verification scores are listed in Table 4.5 below.

	Daytime	Night-time
FAR	0.20510	0.41280
POD	0.59356	0.62414
BIAS	0.74672	1.06292
CSI	0.51472	0.43380

**Table 4.5:** Table of verification scores for daytime and night-time values, separately.

It can be seen from Table 4.5 that FAR is better in the daytime, and on the other hand, POD is better in the night-time. FAR is better in the daytime because the

number of hits is much larger than the number of false alarms. This is due to the overall large number of Cb clouds in the daytime. The number of misses is much larger in the daytime, which affects POD negatively. The big number of misses can be a result of overobservation by a human observer. In addition, observers can easily detect Cb clouds over the detection radius in the daytime. The results also imply that Cb clouds are slightly overdetected by radar in the night-time as the bias is over one. In the daytime, the bias is far under one, which implies underdetecting. This big difference in bias can be due to darkness since a human observer is less likely to overdetect Cb clouds at night-time as visibility is weaker. It is also possible that a human observer is not able to detect every Cb in the night-time, which leads the value of bias to be over one. CSI is better in the daytime due to a large number of hits.

Next, different years and months can be compared together. First, it is calculated if there are any differences in detection accuracy between different years. Different values and verification scores for different years are listed in Table 4.6 below.

	2016	2017	2018	2019	2020
Cb was observed by human and radar (hits)	246	276	234	244	363
Cb was observed only by human (misses)	153	210	210	162	168
Cb was observed only by radar (false alarms)	150	111	72	86	96
Cb was not observed by human or radar (correct negatives)	3862	3817	3899	3905	3783
FAR	0.3787	0.2868	0.2352	0.2606	0.2091
POD	0.6165	0.5679	0.5270	0.6009	0.6836
BIAS	0.9924	0.7962	0.6891	0.8128	0.8644
CSI	0.4480	0.4623	0.4534	0.4959	0.5789

**Table 4.6:** Table of values and verification scores separately by year

Some conclusions of the scores can be drawn from Table 4.6. The largest and therefore the worst FAR as well as the worst CSI are in 2016. This is caused by a large number of false alarms that affect FAR and CSI negatively. The best FAR is in the year 2020 and the second best is in the year 2018, which can be explained with a relatively low amount of false alarms compared to hits. In the year 2020 POD and CSI values are also the best, which means those values are closest to one. The worst POD value is in the year 2018, which can be explained by a large number of misses compared to hits. Somewhat surprisingly, POD is the second-best in the year 2016. This can be explained by the small total number of observed Cb clouds in METARs in 2016. The same reason also affects POD in the year 2019.

Bias is closest to one in 2016 and the furthest from one in 2018. This does not

say anything about the detection accuracy of the results. Instead, it can tell about overdetecting or underdetecting Cb clouds. Bias value of under one means underdetecting Cb clouds, which can be considered to be dangerous for aviation. However, it is likely that human observers have been overeagerly detecting Cb clouds which leads to large number of misses and therefore bias is under one.

Differences between each year are somewhat challenging to explain. Nevertheless, some things affect verification scores. First, the total number of Cb clouds per each year is different, which is due to different weather each year. Observation practices have been the same for over five years, so, likely, they are not affecting the results (Tikkamäki, 2020). However, different people see things differently and have different insights. Moreover, it is possible that the algorithm has been improved on detecting Cb clouds over the years. This would likely be the explanation why detection accuracy was the best in the year 2020.

	June	July	August
Cb was observed by human and a radar (hits)	299	589	475
Cb was observed only by human (misses)	286	343	274
Cb was observed only by radar (false alarms)	144	182	189
Cb was not observed by human or radar (correct negatives)	6448	6321	6497
FAR	0.3250	0.2360	0.2846
POD	0.5111	0.6319	0.6341
BIAS	0.7572	0.8272	0.8865
CSI	0.4101	0.5287	0.5063

**Table 4.7:** Table of values and verification scores separately by month.

Then, different months are compared together. These values are illustrated in Table 4.7 above. It can be seen that June is the only month where the amount of Cb clouds observed only by human (misses) and by human and radar (hits) are very close to each other. This results in decreased POD. In other months, hits are much larger than misses. The best POD and bias are in August, whereas the best FAR and CSI are in July. In June, all verification scores have the worst values. This can be due to the fact that in June there is also the smallest number of Cb clouds observed in total. To summarize monthly variability, the best detection accuracies are in July and August, when CSI values have been the largest. It is hard to conclude which one of these two months have the best accuracy since POD and CSI are so close to each other. However, the bias is closer to one in August, which indicates that the number of times Cb clouds were observed by human and detected by the algorithm are closer to each other.

All code that was used in this thesis can be found in the following Github repository: <https://github.com/lauratuomola/cb-cloud-detection>.

## 4.1. Case examples

Different kinds of case examples are introduced to help to understand different weather situations. First, there is a clear example of a case when both the radar and the observer have observed Cb. In Figure 4.2 below, a case is illustrated, when the detection algorithm has detected Cb. There is a circle with a radius of 20 kilometres in Figure 4.2, and it marks the area where the algorithm is detecting Cb clouds. Cb areas are marked with red and towering cumulus areas marked with blue on the left side of the figure. The radar reflectivity factor is presented on the right side of the figure.

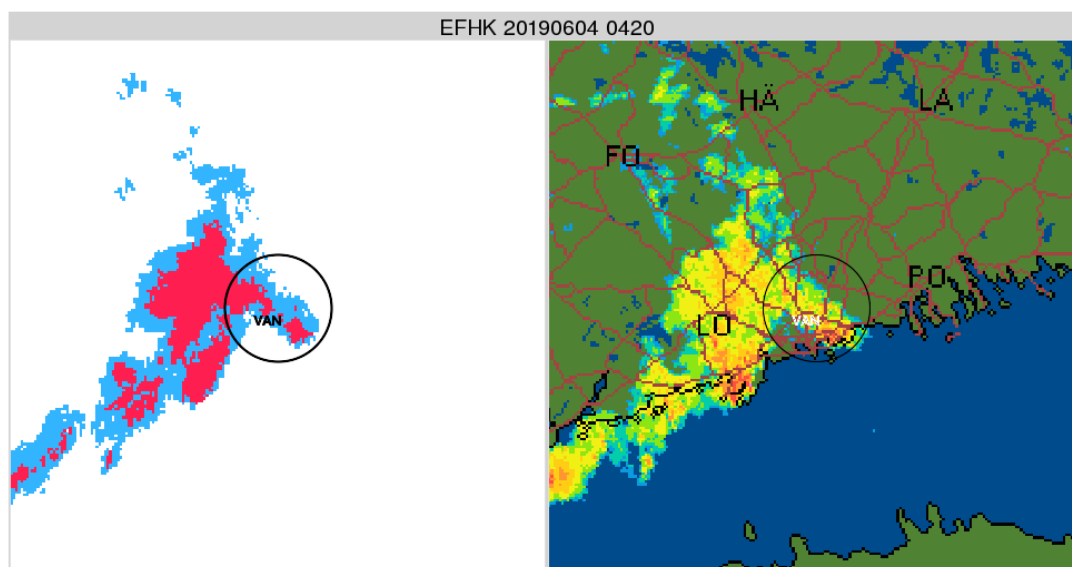


**Figure 4.2:** An example of a case where a radar and observer has observed Cb. Date: the 4th of June 2019 at 04:20 UTC.

METAR for that specific time was EFHK 040420Z 22019KT 9999 -SHRA SCT060CB BKN120 17/12 Q1014 TEMPO 7000 TSRA=, so there is clearly a Cb cloud in both the radar and manual observations.

The second example is from a case when the observer observed Cb cloud, but the radar could not detect it. This case example shows the reason why both 15 and 20 minutes past the hour, as well as 45 and 50 minutes past the hour, measurements were taken into account when deciding if the radar has detected Cb or not. Figure 4.3 below

represents the situation from the radar point of view. It can be seen that the radar did not detect Cb within the radius of 20 kilometres at 20:50 UTC.

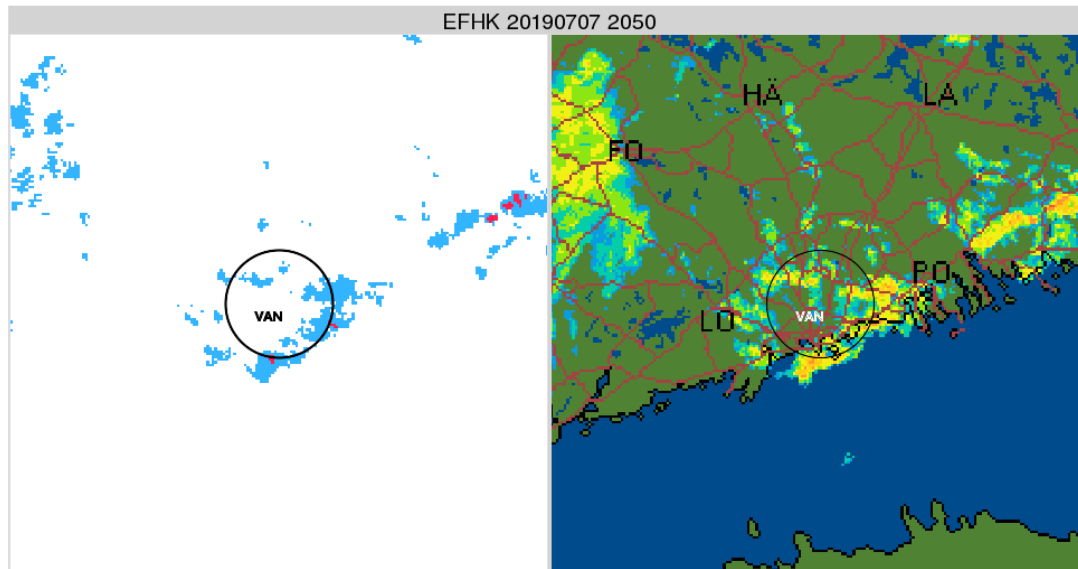


**Figure 4.3:** An example of a case where the observer observed a Cb cloud, but the radar did not detect it. Date: the 7th of July 2019 at 20:50 UTC.

METAR for that time was EFHK 072050Z 36006KT 9999 -SHRA SCT030CB 13/12 Q1000 NOSIG=. From the METAR, it can be seen that the human observer did detect Cb, whereas the radar did not. This case is due to the different timings between radar and human detection. The official METAR observation time is the past 10 minutes before METAR must be sent. If the radar observations at 20:45 UTC are studied, it can be seen in Figure 4.4 below that then the radar detected Cb within the radius of 20 kilometres. This likely caused the difference in this case. This supports the decision why it was important to include both 15 and 20 minutes past the hour and 45 and 50 minutes past the hour measurements in this study to determine if the weather radar detected a Cb cloud.

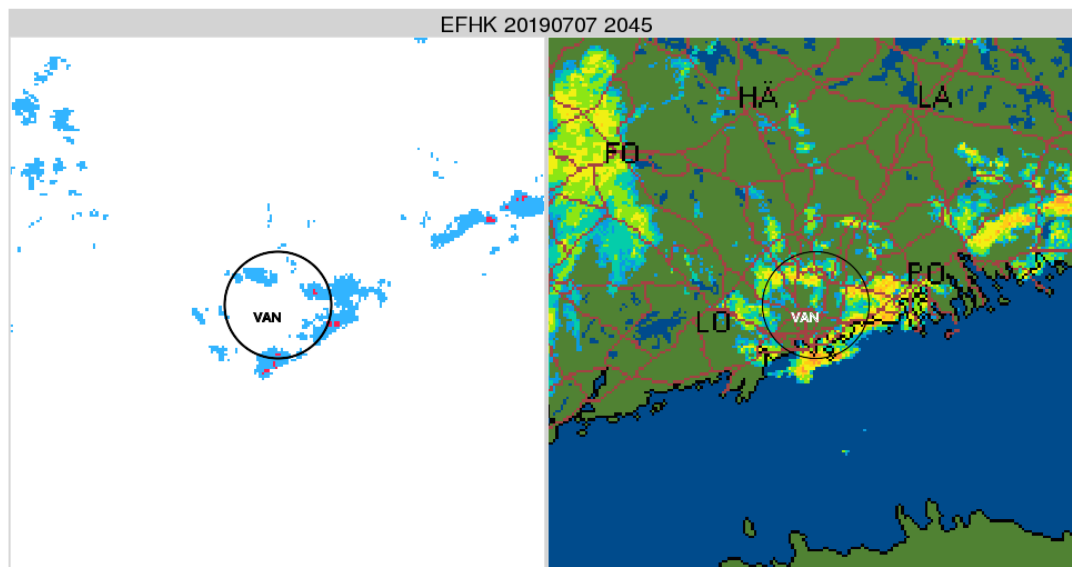


**Figure 4.4:** Date: the 7th of July 2019 at 20:45 UTC.

The following case example is from a situation where the observer detected Cb, but the radar did not. Figure 4.5 represents the situation from the radar's point of view. It can be seen that the radar did not detect Cb within the radius of 20 kilometres. METAR for that time was `EFHK 210850Z 17014KT 9999 SCT018 FEW020CB 19/14 Q1021 NOSIG=`. From this, it can clearly be seen that the human observer detected Cb.

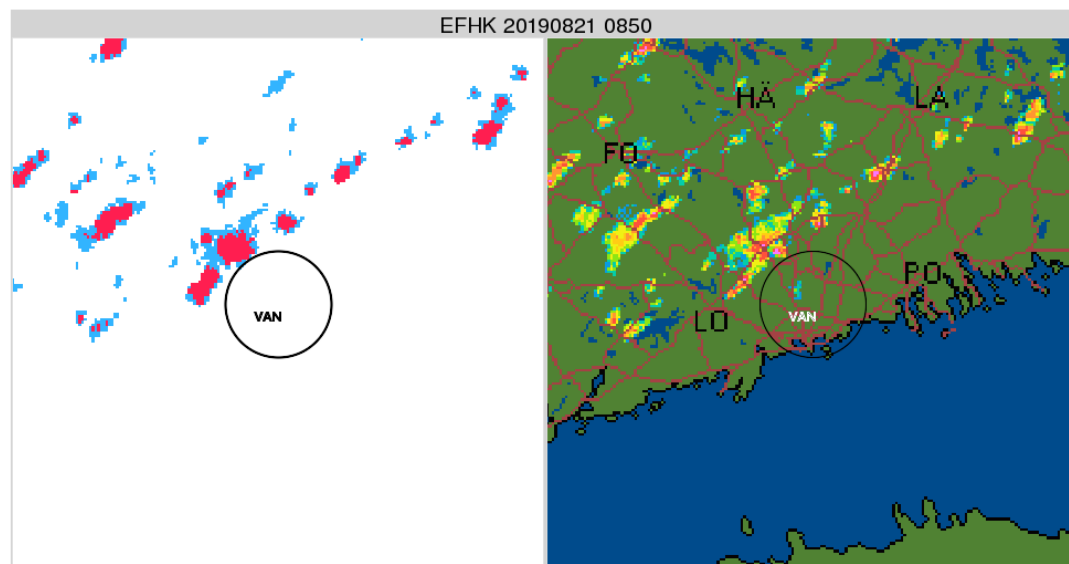


**Figure 4.5:** An example of a case where the observer observed a Cb cloud, but the radar did not detect it. Date: the 21th of August 2019 at 08:50 UTC.

In this specific Cb detection case, the difference between the radar and observer could be due to different detection radii. The radius of the radar detection is precisely defined to be 20 kilometres, whereas a human observer can detect a Cb cloud from a little bit



further distance if it is significant for aviation. It can be seen in Figure 4.5 that the radar has detected a Cb cloud just outside of the 20-kilometre radius, so this is likely the case. The radar has not detected Cb in previous scans either, so it is unlikely that this difference would be due to the different timings.

The fourth example is from a case when the observer could not observe a Cb cloud, but the radar detected it. Figure 4.6 represents the situation from a radar's point of view.

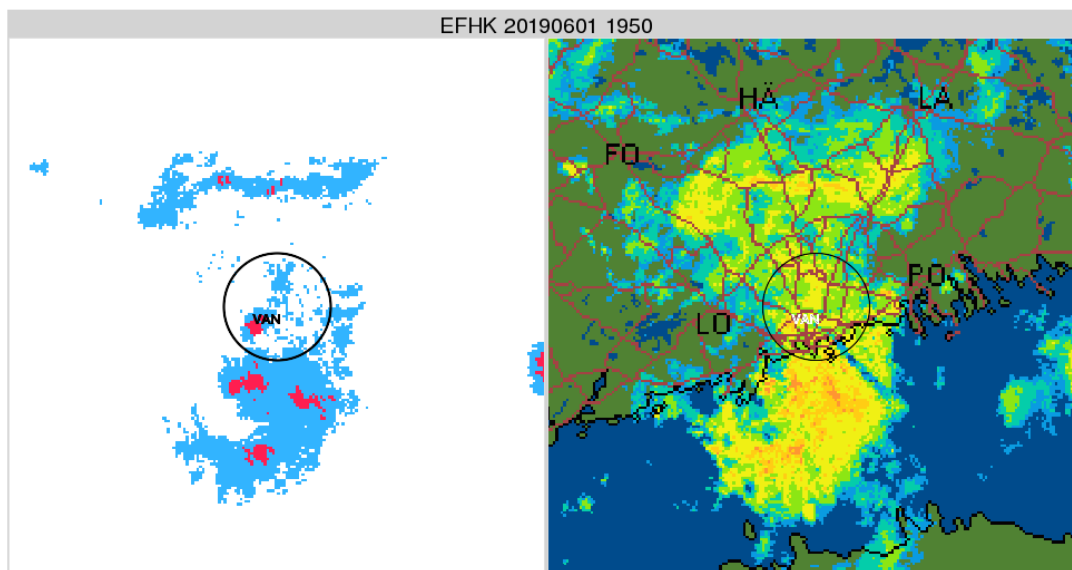


**Figure 4.6:** An example of a case where the radar detected a Cb cloud, but the observer did not. Date: the 1st of June 2019 at 19:50 UTC.

METAR for that specific time was EFHK 011950Z 19009KT 9999 -RA FEW035 BKN040 BKN070 11/09 Q1009 NOSIG=. This tells that the observer did not detect a Cb cloud. In this case, the difference between the radar detection and human observation could be due to a cloud layer. From the METAR it can be seen that there has been few clouds (1-2 octas) of which base was in the height of 3500 feet (FEW035) and lots of clouds (6-7 octas) of which base was in the height of 4000 feet (BKN040) and 7000 feet (BKN070). This suggests that there could have been a cloud layer where a Cb cloud was embedded; therefore, it was difficult for the observer to see it. This specific case was at 19:50 UTC, which means that in Vantaa, Finland the Sun has set about twenty minutes before that on 1st of June so the darkness could also have had an impact.

The fifth example is another case when the radar detected a Cb cloud, but the human observer did not. The situation in Figure 4.7 is represented from a radar's point of view.

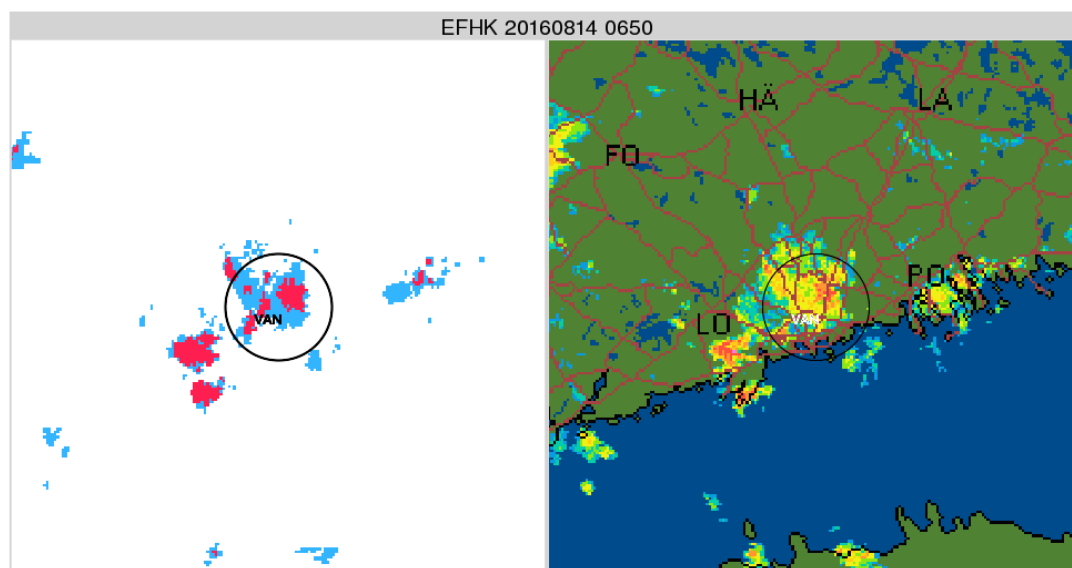


**Figure 4.7:** An example of a case where the radar detected a Cb cloud, but the observer did not. Date: the 14th of August 2016 at 06:50 UTC.

METAR for the specific time was `EFHK 140650Z VRB04G17KT 3500 +TSRA BKN010 15/15 Q1007 BECMG 8000 BKN015=`. From this, it can be seen that the observer did not detect Cb, whereas the radar clearly did. However, thunderstorm (TS) is marked in the METAR. This indicates that there has happened a mistake, meaning that the observer forgot to put Cb in the METAR because thunderstorms are always associated with a Cb cloud. The observer has marked Cb in the next METAR: `EFHK 140720Z 04006KT 8000 TSRA FEW004 BKN040CB 15/14 Q1007 TEMPO 5000 TSRA BKN030CB=`. This supports the assumption that the observer made a mistake and forgot to put Cb in the earlier METAR. There are not many cases like this per year. For instance, there were altogether two cases like this in the dataset of this study. However, this shows that observers are only humans after all and can make mistakes.

Last case example is from another situation where the radar detected Cb, but the observer did not. Figure 4.8 illustrates the situation from a radar's point of view. On the right side of the image, it can be seen that there is no precipitation anywhere on the map. Likely, the detected Cb clouds are not clouds but instead some clutter. METAR for that time was `EFHK 010020Z 24006KT CAVOK 07/05 Q1015 NOSIG=`. The METAR shows that the weather was very clear because there were not any showers or significant clouds and visibility was over 10 000 metres (CAVOK). This supports the assumption that the radar has observed something else than a Cb cloud. For instance, the clutter can be from insects, birds, chaff, the Sun or radio interference.

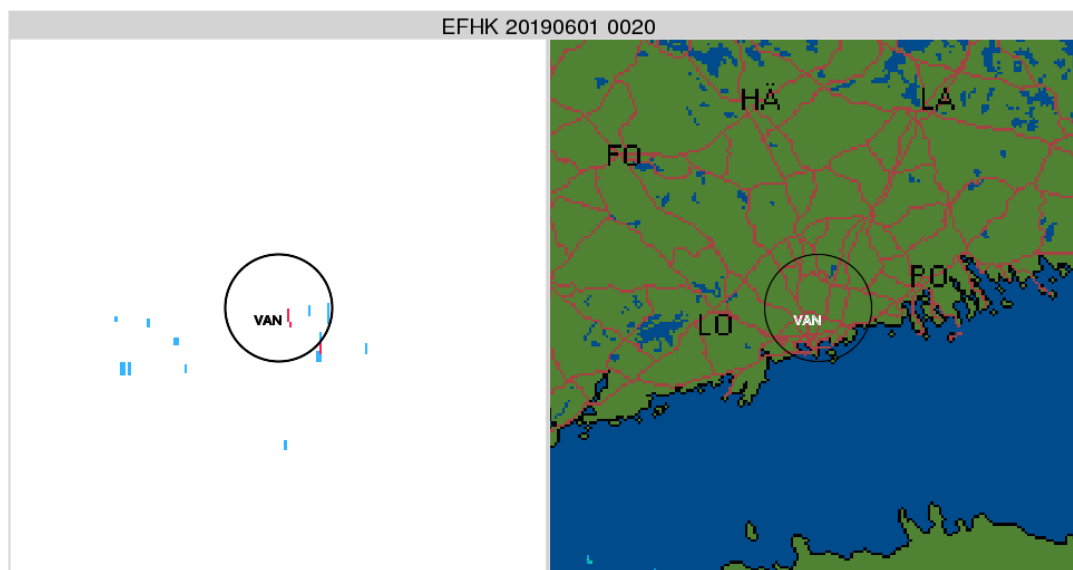


**Figure 4.8:** An example of a case where the radar detected a Cb cloud, but the observer did not. Date: the 1st of June 2019 at 00:20 UTC.

As the last example pointed out, sometimes weather radars can detect Cb even when there is none. The algorithm is fixed so that the lowest elevation angles can be excluded in order to remove residual ground clutter (Hyvärinen et al., 2015). It is still possible that some clutter remains, for example, from sea, birds, insects, wind turbines or chaff (Rauber & Nesbitt, 2018).

The cases included examples of situations where radar detected a Cb cloud, but the observer did not and vice versa. Cases where radar detected Cb but observer did not included difficult conditions such as darkness and embedded Cb, for example, in a frontal system. Cases where a human observer detected Cb but the radar did not are possible, for example, due to different detection radii. Note that there are also other reasons for a contradiction between radar detection and human observation that were not discussed in the case examples. Observers at Helsinki-Vantaa have each their own opinions and insights of the present atmospheric situation when detecting Cb clouds, and sometimes a Cb cloud can easily be obscured by other cloud types.

Some of the algorithm's falsely detected Cb clouds could be due to heavy precipitation caused by some other cloud type. That is not a big mistake from the safety point of view since heavy precipitation can cause harm to aviation regardless of the cloud type. It can cause a reduction of visibility, and the standing water on a runway can affect braking action. Therefore, heavy precipitation must be taken into account in flight planning, even if it is not from Cb. However, Cb clouds cause more severe weather hazards, such as icing, turbulence, hail, strong updrafts and downdrafts, but it is better to be overcautious since people's lives can be affected.

## 4.2. Future steps

In the future, the aim of FMI could be to automatise Cb detection and current weather observation fully, but before that, the algorithm needs to be improved. One approach could be to add satellite observations to improve detection accuracy. These kinds of systems are used in different countries around Europe, for example, in the Netherlands (De Valk & van Westrhenen, 2015) and Germany (Kober & Tafferner, 2009). Matthee & Mecikalski (2013) conducted a study to investigate cloud top infrared fields to find out the physical properties of convective cells. The study was done in Africa near the Equator, so results are probably not valid as such as the dynamics in the atmosphere are different, but similar methods could be used in Finland, too. According to Mueller et al. (2018), satellite observations cannot be used alone without other observation sources because even though the probability of detection is quite high, False Alarm Rate and CSI are not sufficient. Mueller et al. (2018) found out that NWP filtering is an efficient way to increase detection accuracy when Cb cloud detection is based on satellites.

In addition to satellite observations, lightning observations from the lightning network could be added as lightning is a clear sign of Cb. That is actually already done and used in AUTO METARs in Finland, but the information from the network is not included in this study. Weather radar observations and a lightning detection network are used together in Japan to detect Cb clouds (Japan Meteorological Agency, 2016). A lightning detection network is the only tool that New Zealand uses to detect Cb clouds at airports where an automated system is used (Hartley & Quayle, 2014). Honorè et al. (2010) state that data from the lightning network has been proven to be a beneficial addition to radar observations.

De Valk & van Westrhenen (2015) completed a study where they tried to add some values from numerical weather prediction models such as CAPE, CIN and LFC, but the improvement was only marginal. Their conclusion was that if there are advances in the numerical weather prediction models, the improvement might become more significant, and this can become a possibility in the future. In addition, dual-polarization radars have many additional variables that are not yet used at FMI. Rauber & Nesbitt (2018) state that those variables could be used to, for example, discern meteorological and non-meteorological echoes. In addition, the algorithm could be improved by changing the radar reflectivity factor threshold values to see if it has positive effect on verification scores.

## 5. Conclusions

The main goal of this thesis was to analyse the accuracy of the algorithm that detects Cb clouds based on radar observations. It was concluded that it is the best to use measurements from 15 and 20 minutes past the hour and 45 and 50 minutes past the hour from the radar data since it best matches with the ten-minute METAR observation time and provides the best verification scores. The overall scores were satisfactory since the FAR was 0.27, the POD 0.60, the CSI 0.49 and the bias 0.83. CSI was still relatively low, and the scheme as such is not adequate to replace human observers at Helsinki-Vantaa. However, AUTO METARs are already using the algorithm with lightning information to detect Cb clouds at smaller airports in Finland.

Then, differences between daytime and night-time detections were studied and analysed. First, the number of Cb clouds was much higher in the daytime compared to the night-time in both radar and METAR observations. In the daytime, FAR and CSI had better values, whereas POD was better in the night-time and then, also the bias was closer to one. These results are, for instance, due to the large amount of Cb clouds in the daytime as well as the darkness in the night-time. Different months and years were also compared together. It was found out that the best detection accuracy was in the year 2020 and the worst in 2016. Similarly, the best detection accuracy was in July and August when months were compared together. Some reasons to the differences were discussed.

METARs were considered to be the ground truth in this thesis. However, they do not always tell the correct answer in reality. There are several observers working at Helsinki-Vantaa, which means that each observer sees the situation in the atmosphere differently and their own opinions and experiences affects Cb observation. Observers can sometimes detect Cb clouds overeagerly and over the defined detection radius. Sometimes, Cb cloud is embedded in a cloud layer, and also darkness can make Cb detection difficult. All things considered, observations are not precise when humans are observing Cb clouds. It is always based on one's insight into the situation, whereas the radar detection is precise, objective and based on certain threshold values and exact

radius. This difference can have a negative effect on radar detection accuracy in this study, even if the algorithm was working correctly.

Of course, there are downsides in radar detection, too. Even though clutter has been tried to be removed, some of it can still remain as was shown in the case examples. If that was the case, the algorithm would detect Cb even when there is none. Finally, human observations and radar detection are not independent of each other since a human observer uses radar observations to detect Cb clouds, especially in difficult conditions.

In the future, it would be interesting to do a similar kind of study, for example in Rovaniemi, because it is located in the northern part of Finland as the atmosphere is colder there in summer than in Helsinki. Colder atmosphere means that the cloud bases can be lower and more difficult to detect with a radar. In addition, the radar is located further away from the airport in Rovaniemi, which also has an effect on the results. Furthermore, it would be interesting to investigate and compare the differences between two observers from the same airport. Different verification scores could be calculated and see how much they differ.

## 6. Acknowledgements

First of all, I would like to thank my supervisor Jussi Ylhäisi from FMI for useful and helpful comments along the process. Due to coronavirus the situation was not the easiest, but he was always ready to call over Slack whenever I needed. I also would like to thank Antti Lukkarinen and Matti Keränen from FMI who made it possible for me to write my thesis at FMI. In addition, I wish to thank Markus Peura and Harri Hohti from FMI for always answering my questions regarding radars. I would additionally like to thank Marja Bister and Heikki Järvinen for reviewing my thesis. Special thanks to my friends Eevi Laine and Sonja Grönroos who helped me with my English language. Finally, I want to thank my significant other Ville Kopio who encouraged and supported me throughout the thesis.

# Bibliography

- Davidson, M. (1999). Shallow/deep convection. <https://www.wpc.ncep.noaa.gov/international/training/deep/index.htm>. Accessed: 25.09.2020.
- De Valk, P. & van Westrheden, R. (2015). Cb-tcu classification based on radar and satellite observations. *KNMI scientific report*.
- Eastman, R. & Warren, S. G. (2014). Diurnal Cycles of Cumulus, Cumulonimbus, Stratus, Stratocumulus, and Fog from Surface Observations over Land and Ocean. *JOURNAL OF CLIMATE*, 27(6), 2386–2404.
- Emanuel, K. (1997). Overview of atmospheric convection. In R. Smith (Ed.), *The Physics and Parameterization of Moist Atmospheric Convection* chapter 1, (pp. 1–28). Springer Science+Business Media Dordrecht.
- Finnish Meteorological Institute (2020a). *Lentosäähavainto-ohjeet*.
- Finnish Meteorological Institute (2020b). *Lentosääpalvelut Suomessa*.
- Finnish Meteorological Institute (2020c). Sääatutkat. <https://www.ilmatieteenlaitos.fi/avoin-data-saatutkat>. Accessed: 16.12.2020.
- Hartley, B. & Quayle, T. (2014). METAR AUTO Implementation at International Airports in New Zealand. *Meteorological Service of New Zealand Limited*.
- Henken, C. C., Schmeits, M., Wolters, E., & Roebeling, R. (2009). Detection of Cb and TCu clouds using MSG - SEVIRI cloud physical properties and weather radar observations. *KNMI scientific report*.
- Hohti, H. (2020). Private Communication.
- Holton, J. R. & Hakim, G. J. (2012). *An Introduction to Dynamic Meteorology*.
- Honorè, F., Yvagnes, J.-M., & Thomas, P. (2010). Use of lightning data to improve observations for aeronautical activities. *Mètèo-France*.



- Hyvärinen, O., Saltikoff, E., & Hohti, H. (2015). Validation of Automatic Cb Observations for METAR Messages without Ground Truth. *JOURNAL OF APPLIED METEOROLOGY AND CLIMATOLOGY*, 54(10), 2063–2075.
- International Civil Aviation Organization (2018). Meteorological service for international air navigation. *Annex 3 to the Convention on International Civil Aviation*.
- Isolähteenmäki, P. (2020). Private Communication.
- Japan Meteorological Agency (2016). Full automation of aeronautical meteorological observations and reports at aerodromes.
- Jolliffe, I. T. & Stephenson, D. B. (2012). *Forecast Verification: A Practitioner's Guide in Atmospheric Science* (2 ed.). John Wiley & Sons.
- Karttunen, H., Koistinen, J., Saltikoff, E., & Manner, O. (2001). *Ilmakehä ja sää* (3 ed.). Ursan julkaisuja, 62. Tähtitieteellinen yhdistys Ursa.
- Kober, K. & Tafferner, A. (2009). Tracking and nowcasting of convective cells using remote sensing data from radar and satellite. *METEOROLOGISCHE ZEITSCHRIFT*, 18(1), 75–84.
- Leroy, M. (2006). Status of the automatic observation on aerodrome and ongoing improvements in france. *Mètèò-France*.
- Markowski, P. & Richardson, Y. (2010). *Mesoscale Meteorology in Midlatitudes*. John Wiley & Sons.
- Matthee, R. & Mecikalski, J. R. (2013). Geostationary infrared methods for detecting lightning-producing cumulonimbus clouds. *JOURNAL OF GEOPHYSICAL RESEARCH-ATMOSPHERES*, 118(12), 6580–6592.
- Mueller, R., Haussler, S., & Jerg, M. (2018). The Role of NWP Filter for the Satellite Based Detection of Cumulonimbus Clouds. *REMOTE SENSING*, 10(3).
- Nikkanen, T. (2020). Private Communication.
- Rauber, R. & Nesbitt, S. (2018). *Radar Meteorology: A First Course*. John Wiley & Sons.
- Saltikoff, E., Huuskonen, A., Hohti, H., Koistinen, J., & Jarvinen, H. (2010). Quality assurance in the FMI Doppler Weather Radar Network. *BOREAL ENVIRONMENT RESEARCH*, 15(6), 579–594.

Tikkamäki, J. (2020). Private Communication.

Wilks, D. S. (2011). *Statistical Methods in the Atmospheric Sciences*, volume 100 of *International geophysics series*. San Diego: Elsevier Science & Technology.

Woodard, C., Carey, L., Petersen, W., Roeder, W., Gsfc, N., & Afb, P. (2012). Operational utility of dual-polarization variables in lightning initiation forecasting. *Electronic Journal of Operational Meteorology*, 13(6), 79–102.

World Meteorological Organization (2017). International cloud atlas. <https://cloudatlas.wmo.int/en/cumulonimbus-cb.html>. Accessed: 25.09.2020.